SAHLGRENSKA ACADEMY

The value of cardiac MRI texture analysis in patients with clinically suspected myocarditis

M. Sc. Thesis

Evin Ina Papalini

Essay/Thesis:	30 hp
Program and/or course:	Medical Physics
Level:	Second cycle
Semester/year:	Autumn 2018
Supervisor:	Kerstin Lagerstrand
Co-supervisor:	Christian Polte
Examiner:	Magnus Båth

Abstract

Essay/Thesis:	30 hp
Program and/or course:	Medical Physics
Level:	Second cycle
Semester/year:	Autumn 2018
Supervisor:	Kerstin Lagerstrand
Co- supervisor:	Christian Polte
Examiner:	Magnus Båth
Keyword:	Myocarditis, cardiac magnetic resonance, texture analysis

Purpose:
: The aim of this proof-of-concept study was to assess the diagnostic value of texture analysis (TA) based on conventional balanced steady-state-free-precession (bSSFP), late gadolinium enhancement (LGE) and T2-weighted cardiac magnetic resonance imaging (CMRI) in patients with clinically suspected myocarditis.

Method:
: A retrospective cohort study was performed based on 30 patients who underwent a comprehensive CMRI due to clinically suspected myocarditis between 2013 and 2018 at the Sahlgrenska University Hospital: 10 patients with clinical signs and positive myocardial biomarkers (Troponin T, indicating myocardial injury) as well as positive CMRI findings according to Lake Louise Criteria (LLC; group 1), 10 patients with clinical signs and positive myocardial biomarkers but negative CMRI findings according to LLC (group 2), and 10 patients with clinical signs but both negative myocardial biomarkers as well as CMRI findings according to LLC (control group). TA was performed on regions-of-interest, encompassing the left ventricle, on short axis bSSFP, LGE and T2-weighted images using a freely available software package. Promising features were selected to assess their diagnostic potential.

Result:
: The differentiation between group 1 and the control group was possible with the help of three texture features based on bSSFP images (*Variance*: $p = 0.004$, *Gradient Mean*: $p < 0.001$, and *Sum Average*: $p < 0.001$), four texture features based on LGE images (*Variance*: $p < 0.001$, *Skewness*: $p = 0.004$, *Gradient Mean*: $p < 0.001$, and *Sum Average*: $p < 0.001$) and two texture features based on T2-weighted images (*Skewness:* $p < 0.001$ and *Sum Average:* $p = 0.01$).

Conclusion:
: Our results show that TA is feasible based on conventional bSSFP, LGE and T2-weighted CMRI enabling automated detection of myocarditis in patients with initial clinical suspicion, emphasizing the value of bSSFP imaging as a promising non-contrast tissue characterization technique.

Table of content

Abbreviations

CMRI	Cardiovascular magnetic resonance imaging
EMB	Endomyocardial biopsy
LLC	Lake Louise criteria
EGE	Early gadolinium enhanced
LGE	Late gadolinium enhanced
bSSFP	Balanced steady-state-free-precession
TA	Texture analysis
ROI	Regions of interest
RV	Right ventricle
LV	Left ventricle
T2w	T2-weighted imaging
TR	Repetition time
TE	Echo time
GLevNonU	Grey-level nonuniformity
RLNonUni	Run-length nonuniformity
ICC	Intraclass correlation coefficient

1 Background

Myocarditis is a common inflammatory disease of the myocardium [1,2]. The diagnosis remains challenging due to the large spectrum of underlying etiologies and varying clinical presentation. The inflammation is mainly caused by viral infections, but can also be induced by bacterial, fungal and parasitic infections amongst other factors. Other non-infectious causes have been identified, including drugs, radiation and chemicals. The symptoms of the disease are highly variable and range from unspecific, such as fatigue, to common cardiac symptoms like chest pain or arrhythmias. Therefore, myocarditis may clinically mimic other cardiac diseases. In early stages of the disease, known as acute myocarditis, it usually resolves spontaneously but can rarely even cause acute heart failure or life-threatening arrhythmias/sudden cardiac death. Sometimes, however, it may develop into a chronic condition, resulting in end-stage heart disease with a dilated cardiomyopathy. Studies have reported that myocarditis is shown to be responsible for 6-22 % of all cases of sudden cardiac death in young healthy adults. Thus, it is important to find better markers and methods to improve the diagnosis, and hence, the prognosis of myocarditis.

In recent years, cardiovascular magnetic resonance imaging (CMRI) has been recommended for the diagnosis of myocardial tissue diseases, such as myocarditis [3]. Several studies have shown high diagnostic accuracy for CMRI [3], using endomyocardial biopsy (EMB) as reference standard [1]. The overall goal is to replace EMB completely with the non-invasive CMRI method.

The CMRI examination includes different types of imaging techniques that provides functional and morphological, but also tissue characterization information, where pathology as edema, hyperemia, capillary leakage, necrosis and fibrosis associated with myocarditis can be detected [3]. The CMRI diagnosis of myocarditis is currently based on the validated Lake Louise criteria (LLC) where two out of the three following criteria should be fulfilled: 1) visualization of edema on T2-weighted imaging, 2) capillary leak/hyperemia on early gadolinium-enhanced (EGE) T1-weighted imaging, and 3) necrosis/fibrosis on late gadolinium-enhanced (LGE) T1-weighted imaging, based on delayed acquired images.

Acute necrosis and myocardial scar, *i.e.* fibrosis, are detected with LGE imaging, due to the accumulated contrast agent and delayed washout from the myocardial tissue [4]. This results in an increase in extracellular volume due to edema or when necrotic cells are replaced by fibrotic tissue [3]. The increased contrast agent in the injured regions will lead to a high signal on delayed images, acquired with an inversion recovery gradient echo sequence using an inversion time that nulls the signal from normal myocardium [4]. In myocarditis, the myocardial injury appears in the mid wall and/or subepicardium (Figure 1). Hence, the location of the injury in LGE images distinguishes the disease from ischemic causes. Edema itself can be visualized directly with T2-weighted images as a bright signal surrounded by darker normal myocardium.

Balanced steady-state-free-precession (bSSFP) is a pulse sequence that generates T2/T1-weighted images [5]. As such, the images are produced with high signal-to-noise-ratio and the contrast between blood and myocardial tissue is high. Moreover, the technique acquires multiple images over all phases of the cardiac cycle in just one breath-hold and enable robust estimation of cardiac function such as the stroke volume. As the images display T2/T1-weighted contrast, however, they should have the feasibility to offer not only functional information, but also visualization of myocardial injury/scar and/or inflammation.

The diagnosis of myocarditis is based on visual examination of images taken with qualitative techniques, *i.e.* LGE and T2-weighted imaging. However, the images may contain pathological

information that is not visible to the naked eye. Recently, texture analysis (TA) has emerged as a promising CMRI method to quantitatively characterize myocardial tissue and improve the diagnosis of various myocardial diseases. With TA, features are extracted from regions of interests (ROIs) and computed with data-characterization algorithms, based on the distribution of pixels and their grey-level values in an image [6]. Baeßler *et al.* have shown excellent accuracy of TA on non-contrast T1-weighted images in patients with hypertrophic cardiomyopathy [7]. Moreover, Baeßler *et al.* have demonstrated high sensitivity and specificity for the diagnosis of acute myocarditis applying TA on T2-mapping CMRI [8]. Hence, with the use of TA, subtle changes of the tissue can be detected, and the underlying texture of the tissue can be quantified into diagnostic features.

We hypothesize that TA should also have the feasibility to extract diagnostic features in patients with clinically suspected myocarditis using conventional techniques as performed in clinical routine, *i.e.* bSSFP, LGE and T2-weighted imaging. We believe that such texture features can provide quantitative parameters with high accuracy, reflecting injured myocardial tissue in patients with myocarditis, and thus enhance the application of non-invasive CMRI methods.

Hence, the aim of this study was to assess the diagnostic value of TA based on conventional bSSFP, LGE and T2-weighted CMRI in patients with clinically suspected myocarditis.

2 Materials and methods

2.1 Study population

Among all patients that underwent CMRI due to clinically suspected myocarditis between 2013 and 2018 at the Sahlgrenska University Hospital, a subset of patients were randomly selected and grouped into the following three cohorts consisting of 10 patients each: Group 1 – clinical signs of acute myocarditis with positive myocardial biomarkers (Troponin T, indicating myocardial injury) and positive CMRI findings according to LLC, Group 2 – clinical signs of myocarditis with positive myocardial biomarkers but negative CMRI findings according to LLC, and Group 3 – clinical signs but both negative myocardial biomarkers and CMRI findings according to LLC (control group). However, negative results do not exclude the diagnosis. Images with insufficient image quality due to motion artifacts, *i.e.* with non-distinguishable epicardial border, were omitted. Demographics of patients for each group are summarized in Table 1.

The study was conducted according to the Declaration of Helsinki. Ethical approval was given by the Regional Ethics Review Board at the Västra Götaland.

Table 1. Patient demographics.

Parameter	Group 1	Group 2	Group 3	p-value
Age [years]	25 ± 6	33 ± 14	45 ± 15	**0.02**
Females/males (n)	1/9	5/5	1/9	0.21
Height [cm]	180 ± 10	176 ± 7	179 ± 5	0.29
Weight [kg]	83 ± 19	76 ± 18	86 ± 9	0.22

Data are expressed as mean ± standard deviation or number (n). The significance of the differences is indicated as p-values (level of significance $p < 0.05$ (bold)).

2.2 CMRI data acquisition

All CMRI examinations were performed on a clinical 1.5T whole-body Philips MRI scanner (Philips Medical Systems, Best, The Netherlands) using the five-channel cardiac phased array coil.

Conventional imaging had been performed in all patients, including scout imaging, morphological and functional studies of the heart. The scan protocol had been completed within 45 minutes with measurements during breath hold at end expiration, using retrospective electrocardiographic gating. Balanced SSFP imaging was performed in both long axis and short axis views. In this study, however, only bSSFP together with LGE and T2-weighted images in the short axis orientation were used for analysis (Figure 1). Typical sequence parameters for the different techniques are presented in Table 2.
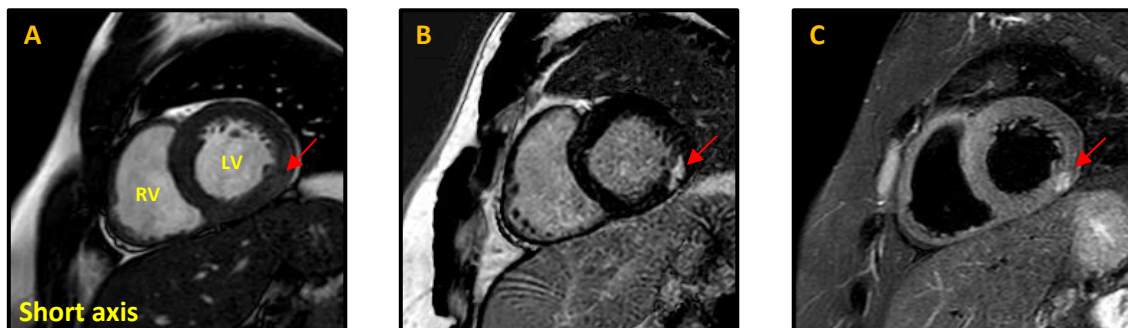

Figure 1. Images of the heart in short axis orientation, obtained with (A) bSSFP, (B) LGE and (C) T2-weighted CMRI. The white areas in the myocardium indicate inflammation due to myocarditis (red arrows). For information, right ventricle (RV) and left ventricle (LV) are also shown.

Table 2. Typical protocol parameters for bSSFP, LGE and T2-weighted CMRI.

Parameter	bSSFP	LGE	T2w
Field of view [mm]	320×320	320×320	350×350
Acquisition Matrix	196×168	196×187	232×181
TR [ms]	2.8	6.1	1714
TE [ms]	1.4	3	70
Slice thickness [mm]	8	8	8
Reconstructed in-plane resolution [mm]	0.61×0.48	0.61×0.58	0.66×0.52
Time frames per cardiac cycle	40	-	-

bSSFP = balanced steady-state-free-precession, LGE = late gadolinium enhancement, T2w = T2-weighted imaging, TR = repetition time, TE = echo time.

2.3 Texture analysis

Texture analysis was performed in all patients using a freely available software package (MaZda version 4.6, Institute of Electronics, Technical University of Lodz, Lodz, Poland) [9-11]. ROIs encompassing the left ventricular myocardium were manually drawn on each exported DICOM-image, as shown in Figure 2. To reduce the risk of partial volume effects, both the trabeculated layer and the epicardial border were excluded. After segmentation, TA was performed using MaZda where the feature computation was completed within a second. In total, 204 images were used, with 63, 78 and 63 images in the three patient groups, respectively.
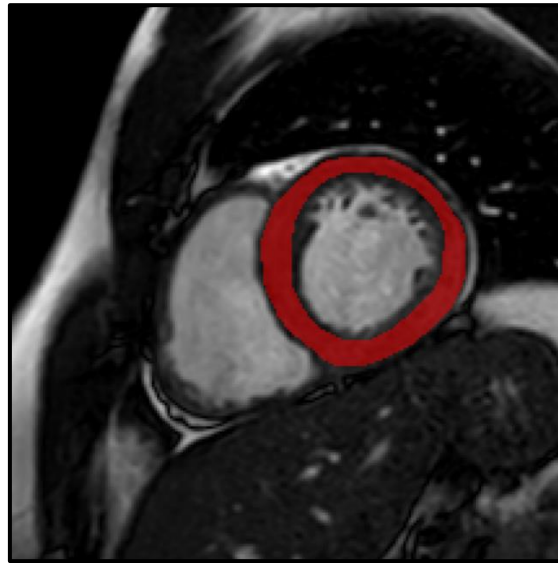

Figure 2. A typical free-hand ROI drawn on a bSSFP image, encompassing the left ventricular myocardium.

Before TA, grey-level normalization was performed by MaZda to correct for small technical intra- and inter-scanner fluctuations and to minimize the effect of contrast and brightness variations. This was obtained by rescaling histogram data to fit within $\mu \pm 3\sigma$ (μ – grey-level mean, σ – grey-level standard deviation).

Six subset texture feature sets were extracted from the segmented region, resulting in 279 texture features based on histogram, absolute gradient, run-length matrix co-occurrence matrix, auto-regressive model and wavelets (Appendix A – Texture analysis). In this study, only 12 promising features, presented in previous studies [7,8], were used (Table 3). The features from the run-length matrix category were calculated in 4 different directions: horizontal (0°), vertical (90°) and angulated at 45° and 135°. The selected features were statistically compared between the different patient groups and imaging sequences.

Table 3. Texture features used for the assessment of their diagnostic potential.

Texture Category	Texture feature	Number of used features
Histogram	Skewness	1
Histogram	Variance	1
Absolute gradient	Gradient Mean (dimensions: 4 bits/pixel)	1
Run-length matrix	GLevNonU (dimensions: 6 bits/pixel, 0°, 45°, 90°, 135°)	4
Run-length matrix	RLNonUni (dimensions: 6 bits/pixel, 0°, 45°, 90°, 135°)	4
Co-occurrence matrix	Sum Average (dimensions: 6x6 bits/pixel, distance: 3)	1

GLevNonU = grey-level nonuniformity, RLNonUni = run-length nonuniformity.

2.4 ROI analysis

To determine the reproducibility of the analysis and investigate the impact of training for the drawing of ROIs, the first 10 individuals were reanalyzed by the same observer, separated in time by approximately 1 week.

2.5 Statistical analysis

All statistical analysis was performed using MATLAB (MATLAB R2018b, The MathWorks, Inc., Natick, MA, USA) [12]. Data are presented as mean ± standard deviation unless stated otherwise. The non-parametric Wilcoxon signed-rank test was used to determine the significance of the difference between the different groups and techniques, where $p < 0.05$ was considered as statistically significant. The agreement in features between repeated measurements was assessed by intraclass correlation coefficient (ICC), where less than 0.40 was considered as poor agreement, $0.40 – 0.59$ was considered as fair agreement, $0.60 – 0.74$ as good agreement and $0.75 – 1.0$ as excellent agreement [13].

3 Results

3.1 Texture analysis

Results from the texture analysis are presented in Table 4 in terms of means and standard deviations. The p-values for all features between group 1-3, 2-3 and 1-2 are presented in Table 5.

Comparing group 1 (patients with both positive myocardial biomarkers and CMRI findings according to LLC) and 3 (controls with both negative myocardial biomarkers and CMRI findings according to LLC), the following four texture features showed statistically significant differences between the groups based on LGE imaging ($p < 0.004$): *Gradient Mean*, *Sum Average*, *Skewness*, *Variance* (Table 5). Except for *Skewness*, these features also differed between the two groups based on bSSFP images ($p < 0.004$). For the T2-weighted imaging, only *Sum Average* and *Skewness* showed significant differences ($p < 0.01$). In Figure 3, the results of the four most important features are illustrated with Box-Whiskers plots for each technique and group.

Comparing patients with clinical signs and positive myocardial biomarkers but negative CMRI findings (group 2) with controls (group 3), *Gradient Mean* and *Variance* were significantly different, however, only for the T2-weighted images. Except for this, the groups could not be differentiated by the four features that were previously shown to be important when comparing group 1 and 3. However, almost all run-length features were significantly different between these groups (Figure 3).

**Table 4.** Calculated means and standard deviations of all texture features in each group and technique.

	Group 1			Group 2			Group 3		
Texture features	bSSFP	LGE	T2w	bSSFP	LGE	T2w	bSSFP	LGE	T2w
Skewness	0.39 ± 0.37	0.94 ± 0.38	0.40 ± 0.37	0.17 ± 0.30	0.66 ± 0.55	-0.01 ± 0.23	0.25 ± 0.31	0.48 ± 0.49	-0.01 ± 0.29
Variance	236 ± 185	1290 ± 1748	706 ± 1143	141 ± 201	243 ± 319	330 ± 451	95.9 ± 96.5	136 ± 141	368 ± 357
Gradient Mean	2.74 ± 0.55	2.24 ± 0.36	2.36 ± 0.45	3.42 ± 0.41	2.95 ± 0.42	2.76 ± 0.48	3.43 ± 0.37	2.87 ± 0.73	2.19 ± 0.49
GLevNonU (0°)	41.1 ± 14.8	48.9 ± 12.4	45.8 ± 11.9	37.7 ± 11.3	38.2 ± 13.7	33.0 ± 9.82	47.8 ± 15.7	58.0 ± 21.1	47.9 ± 16.5
GLevNonU (45°)	42.2 ± 15.0	50.5 ± 12.5	47.6 ± 12.5	38.9 ± 11.8	39.4 ± 14.2	34.2 ± 10.0	48.6 ± 15.9	61.1 ± 25.2	50.5 ± 17.3
GLevNonU (90°)	40.9 ± 14.7	47.9 ± 11.8	46.2 ± 12.0	38.1 ± 11.3	38.1 ± 13.7	33.4 ± 9.76	47.4 ± 15.6	57.9 ± 21.5	48.6 ± 16.4
GLevNonU (135°)	42.3 ± 15.2	50.4 ± 12.7	47.8 ± 12.6	39.3 ± 11.9	39.1 ± 13.9	34.2 ± 10.1	48.6 ± 16.0	61.8 ± 27.8	50.8 ± 17.5
RLNonUni (0°)	995 ± 209	1166 ± 272	1244 ± 312	810 ± 235	861 ± 260	837 ± 214	960 ± 226.7	1170 ± 512	1272 ± 451
RLNonUni (45°)	1053 ± 210	1241 ± 291	1352 ± 344	871 ± 253	926 ± 278	916 ± 226	1014 ± 237	1271 ± 565	1428 ± 485
RLNonUni (90°)	972 ± 196	1117 ± 263	1252 ± 305	824 ± 238	852 ± 254	858 ± 209	942 ± 212	1177 ± 533	1309 ± 430
RLNonUni (135°)	1050 ± 216	1243 ± 293	1365 ± 355	893 ± 271	918 ± 272	917 ± 221	1008 ± 229	1269 ± 564	1440 ± 495
Sum Average	64.5 ± 1.30	66.2 ± 1.27	64.7 ± 1.61	63.3 ± 1.36	64.1 ± 1.93	64.1 ± 1.32	62.8 ± 0.88	63.3 ± 1.54	63.7 ± 0.76

bSSFP = balanced steady-state-free-precession, LGE = late gadolinium enhancement, T2w = T2-weighted imaging, GLevNonU = grey-level nonuniformity, RLNonUni = run-length nonuniformity. Texture features are dimensionless.

Table 5. Estimated p-values for all texture features between group 1-3, 2-3 and 1-2.

Texture feature	Group 1-3			Group 2-3			Group 1-2		
	bSSFP	LGE	T2w	bSSFP	LGE	T2w	bSSFP	LGE	T2w
Gradient Mean	**< 0.001**	**< 0.001**	0.2	0.9	0.8	**< 0.001**	**< 0.001**	**< 0.001**	**0.004**
Sum Average	**< 0.001**	**< 0.001**	**0.01**	0.2	0.3	0.3	**0.005**	**< 0.001**	0.1
Skewness	0.3	**0.004**	**< 0.001**	0.4	0.3	0.7	**0.05***	0.03	**< 0.001**
Variance	**0.004**	**< 0.001**	0.5	0.5	0.2	**0.04**	0.01	**< 0.001**	0.01
GLevNonU (0°)	0.2	0.2	0.9	**0.02**	**< 0.001**	**< 0.001**	0.6	**0.009**	**< 0.001**
GLevNonU (45°)	0.2	0.2	0.9	**0.04**	**0.001**	**< 0.001**	0.6	**0.009**	**< 0.001**
GLevNonU (90°)	0.2	0.1	0.9	**0.04**	**< 0.001**	**< 0.001**	0.6	0.01	**< 0.001**
GLevNonU (135°)	0.2	0.2	0.9	0.05	**< 0.001**	**< 0.001**	0.6	**0.008**	**< 0.001**
RLNonUni (0°)	0.7	0.9	0.8	**0.02**	**0.006**	**< 0.001**	**0.003**	**< 0.001**	**< 0.001**
RLNonUni (45°)	0.7	0.9	0.8	**0.04**	**0.006**	**< 0.001**	**0.005**	**< 0.001**	**< 0.001**
RLNonUni (90°)	0.8	0.7	0.9	0.06	**0.006**	**< 0.001**	**0.008**	**0.002**	**< 0.001**
RLNonUni (135°)	0.7	0.9	0.7	0.08	**0.005**	**< 0.001**	0.01	**< 0.001**	**< 0.001**

bSSFP = balanced steady-state-free-precession, LGE = Late gadolinium enhancement, T2w = T2-weighted imaging, GLevNonU = grey-level nonuniformity, RLNonUni = run-length nonuniformity. Statistically significant p-values are highlighted in **bold** (p < 0.05). * Indicates that p-values were rounded up to 0.05.
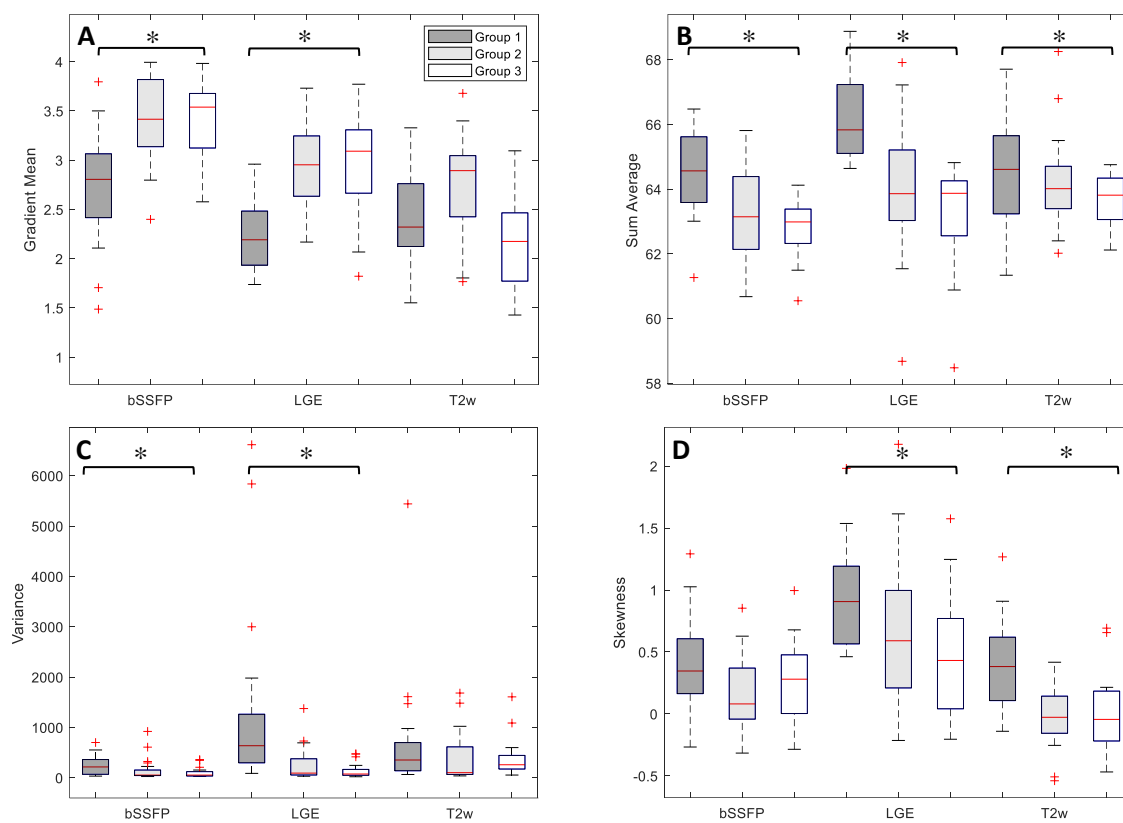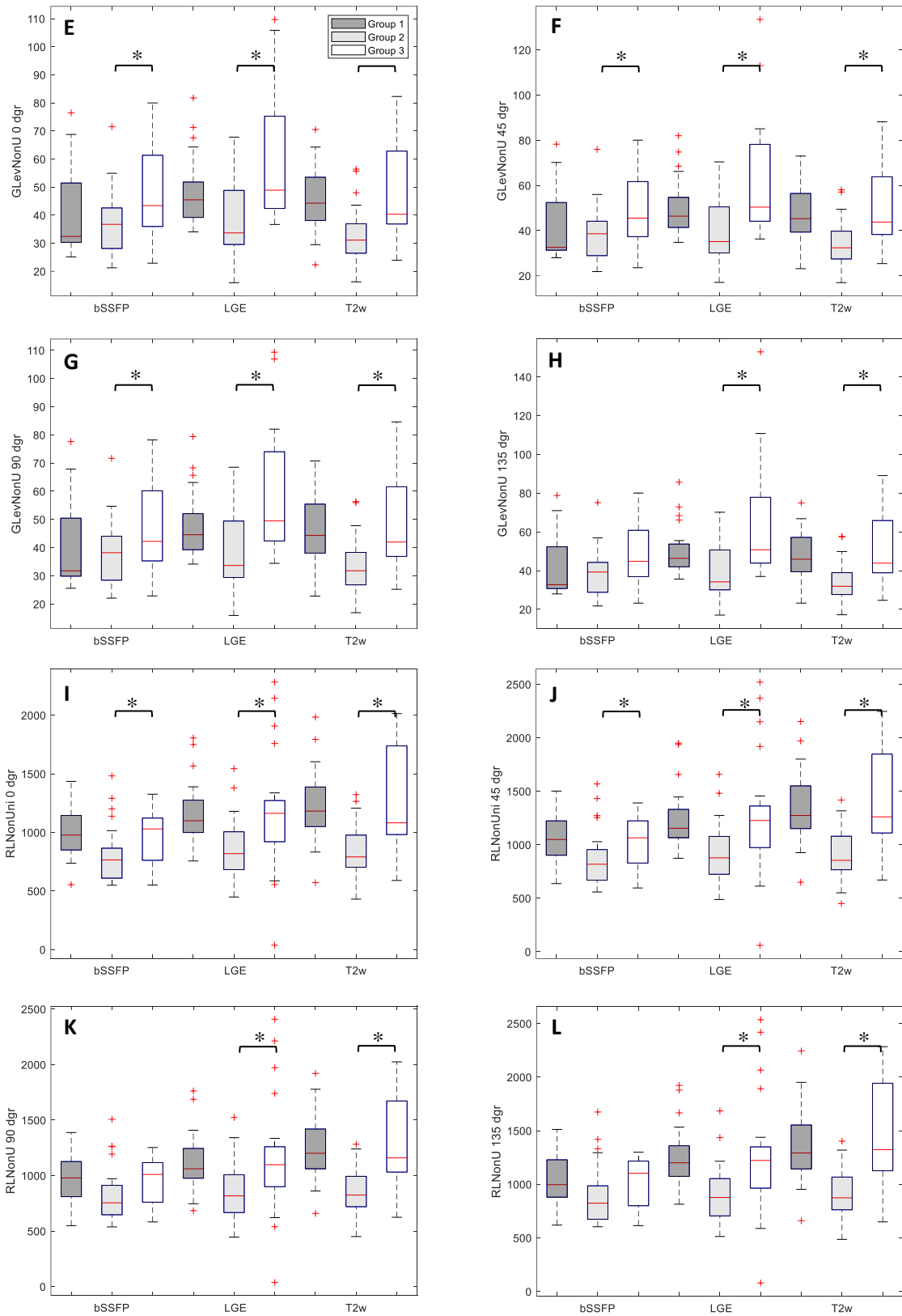
Figure 3. Box-Whisker plots illustrating the differences for texture features between group 1 (dark grey), 2 (light grey) and 3 (white) in bSSFP, LGE and T2-weighted images. The important features are shown in (A) to (D) with significant difference between group 1 and 3. Run-length features are presented in (E) to (L), showing significant difference between group 2 and 3. The median is represented by the centerline of the boxplot with upper and lower limits of 25th and 75th percentiles, respectively. The Whiskers extending from the boxes indicates the most extreme values within 25th and 75th percentiles ±1.5*interquartile range; data points beyond the whiskers are displayed as +. Texture features are dimensionless. * Indicates statistically significant p-values (p < 0.05). bSSFP = balanced steady-state-free-precession, LGE = Late gadolinium enhancement, T2w = T2-weighted imaging, GLevNonU = grey-level nonuniformity, RLNonUni = run-length nonuniformity.

3.2 ROI analysis

For all features extracted from the bSSFP, LGE and T2-weighted images in the reanalyzed patients, the ICC-values were generally in the range 0.6–1.0, indicating good or excellent agreement regarding the reproducibility (Table 7, Appendix – Supplementary results). Figure 4 illustrates the small impact of ROI training on TA for bSSFP (A), LGE (B) and T2-weighted (C) images, in *Gradient Mean*. Similar results were found concerning the other features (not presented).
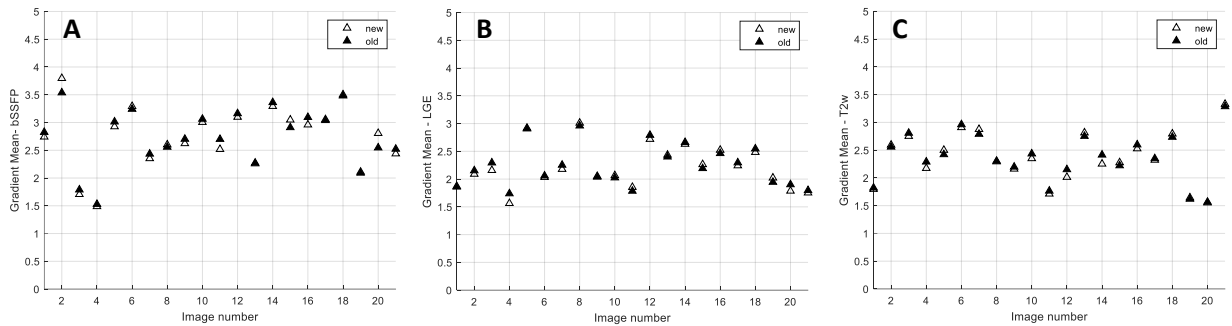

Figure 4. The ROI analysis shows no impact of training for the drawing of ROIs in the bSSFP (A), LGE (B) and T2-weighted (C) images (x-axis) of *Gradient Mean* (y-axis), demonstrating good/excellent agreement of the old measurement and new (repeated) measurement. Similar results were found concerning the other features. Texture features are dimensionless. bSSFP = balanced steady-state-free-precession, LGE = Late gadolinium enhancement, T2w = T2-weighted imaging.

4 Discussion

In this study, the potential of TA based on conventional bSSFP, LGE and T2-weighted CMRI was investigated for the purpose of differentiating between groups of patients with and without clinical signs of myocarditis using myocardial biomarkers and the LLC as reference standard. Moreover, groups of patients with and without CMRI findings of myocarditis were also compared to see if TA can find pathological patterns, present in the image but not directly visible for the eye. The main findings of the study were that TA is highly feasible using bSSFP, LGE and T2-weighted CMRI and delivers texture features that allow the successful differentiation between the presence and absence of myocarditis in a patient (group 1 versus 3). Hence, TA is a promising tool that enables automated detection of myocarditis and obtains quantitative information with high diagnostic accuracy. Further investigations are needed to determine the true additional value of using combined features and techniques to improve the diagnosis of myocarditis on an individual patient level.

The strongest texture features for the differentiation between group 1 (both positive myocardial biomarkers and CMRI findings proving the presence of myocarditis) and 3 (both negative myocardial biomarkers and CMRI findings proving the absence of myocarditis) were *Variance*, *Skewness*, *Gradient Mean* and *Sum Average*. All these features showed high statistical significance on LGE images. The bSSFP imaging technique could also separate these features, except for *Skewness*. With T2-weighted imaging, however, only *Sum Average* and *Skewness* were significantly different between the two groups. This was probably due to the lower contrast between normal and injured myocardium in these images.

Although a previous report has shown high sensitivity and specificity for T2-maps in detecting acute myocarditis [8] using features from the run-length matrix, we found no significant features from this category in our study when differentiating between patients in group 1 and controls in group 3. There are several ways of explaining this. In the present study, we did not use the same imaging technique as in the previous study that used advanced T2-mapping. As such, the images presented pure T2-weighting and no T1-weighted contrast as conventional T2-weighted images. Additionally, the technique may have offered higher image quality, sufficient for TA. A more likely explanation is that our control group did not contain entirely healthy volunteers. The individuals had clinically suspected myocarditis, but with negative myocardial biomarkers and CMRI findings. Thus, myocarditis was excluded based on current standard techniques as in clinical routine. Nonetheless, we cannot completely exclude the fact that some of these individuals might have had undetected myocarditis, with false negative biomarkers and CMRI, and/or had another unknown heart disease, which might have negatively affected the analysis. Most importantly, our control group (mean age 45 ± 15 years) was probably older than the group in the previous study. The age of the controls was not listed in the article, but it is reasonable to assume that the group consisted of young healthy students. As the myocardial tissue degenerates with age [14], changes in image characteristics measured by TA may appear. This could explain the patchiness in the myocardium of our control group that was observed after an inspection of the images. As such, the run-length features are presumably sensitive to small changes in tissue characteristics and will therefore present similar values for the patients with myocarditis as for the controls. Moreover, healthy students have less problems with arrhythmia and tend to be more willing to cooperate. This should give the control cohort of the previous study lower artefactual level of the images.

Comparing patients in group 2 (positive myocardial biomarkers but negative CMRI findings) and controls in group 3, *Gradient Mean* and *Variance* showed significant differences between groups, however, only for the T2-weighted images. Except for this, the features that were found to be strong markers of myocarditis, *i.e. Variance*, *Skewness*, *Gradient Mean* and *Sum Average*, did not discriminate

between these two groups. On the other hand, all run-length features did. Features derived from the run-length matrix are based on the computation of number of runs of pixels, of a given length, with the same grey-level value [6,15,17]. A grey-level run is a set of adjoining pixels with the same grey-level value, and the grey-level run-length represents the number of pixels in it. The distribution will give the total number of runs for each grey-level value, meaning the distribution will be large when the runs are not homogenously distributed over the different grey-levels. Thus, *GLevNonU* and *RLNonUni* are describing the homogeneity of the grey-level distribution and should obtain lower values if the texture is homogenous, as in normal myocardial tissue. In this study, the myocardium in group 3 was not completely homogenous, as already discussed. Also, we noticed that the images in group 2 were more smoothed than others, therefore, the run-length features generally displayed lower values in this group. Such smoothing could be explained by arrhythmic behavior.

Both *Variance* and *Skewness* were expected to give significant differences between group 1 and 3 as the measures reflect differences in heterogeneity for the entire myocardial ROI. These features are derived from the histogram of an image, where the histogram represents the distribution of pixels with a given grey-level value [6]. The variance describes the spread out from the mean of the grey-level values and the skewness describes the asymmetry of the distribution of the grey-level values, where a positive skewness indicates a longer tail to the right (higher intensity values) [6,15]. In bSSFP, LGE and T2-weighted images, pathology will appear with high intensity values, leading to a larger variance and a longer tail to the right of the distribution, hence positive skew. Our results showed higher values for *Variance* and *Skewness* in group 1 compared to group 3 for all imaging techniques (Table 4), but *Variance* was only significant for LGE and bSSFP imaging, while *Skewness* only was significant for LGE and T2-weighted images. Thus, high values in *Variance* and *Skewness* may indicate pathology and might be good discriminators using LGE images. The higher values of these features in LGE imaging can be explained by the high contrast between diseased and normal myocardium, provided by the inversion time of the inversion recovery gradient echo sequence that nulls the signal from normal tissue, and the contrast agent that enhances the signal from the injured tissue [4]. In bSSFP imaging, the contrast depends on the T2/T1 ratio, resulting in a good contrast between the blood and myocardium [5], but not as good between normal myocardium and pathology as in LGE. Furthermore, if edema is present, the contrast in T2-weighted images will be high between the inflamed and normal tissue [3], changing the distribution of the histogram with higher values of *Skewness* than in bSSFP images, as shown by our results. The contrast was, however, not sufficient to give significance in *Variance* since the grey-level distribution within the myocardium displayed a small range from light grey to white and not as in LGE where the grey scale varies from black to white. With these statements, LGE imaging was considered as the best technique in differentiating between group 1 and 3. For group 1, this technique differed significantly from bSSFP imaging for most features (Table 6, Appendix – Supplementary results), except for *RLNonUni* in the directions 0°, 90° and 135°.

The gradient based feature, *Gradient Mean*, was expected to separate group 1 from 3, as it is a measure of the spatial variation of the grey-level values in an image [6], that will change when pathology is visible or not. The *Gradient Mean* feature showed lower average values for group 1 compared to group 3, which might be explained by quenching of the gradient vectors in areas with pathology, due to the high signal intensity. Nonetheless, the older controls in group 3 had slightly patchy myocardium. That is, more gradients will contribute to the gradient mean of the ROI.

At last, *Sum Average* was expected to be a good discriminator as it is a measure of the heterogeneity in the ROI. The feature is derived from the co-occurrence matrix that contains information about the grey-level distribution of pairs of pixels and is calculated as the mean of the sum of this distribution [15]. As pathology is present, there will be occurrences of pairs of pixels with more combinations of

grey-level values, giving a larger distribution and therefore a higher value of *Sum Average*. Comparing group 1 and 3, this feature showed high statistical significance in all three imaging techniques.

Our results yielded another interesting finding regarding the value of bSSFP imaging technique for the diagnosis of myocarditis. To our knowledge, no other studies have previously investigated the value of bSSFP imaging for the diagnosis of myocarditis and no study has used advanced analysis tools for automated diagnosis of myocarditis from bSSFP images. As seen from our results, the technique might be used as a surrogate to LGE for the detection of myocarditis. This finding is very satisfying, since bSSFP imaging offers a non-invasive non-contrast medium alternative to LGE. The bSSFP imaging technique may not have the possibility to replace LGE completely, although the combination of these techniques could increase the diagnostic potential of TA. As stated before, LGE appears bright on delayed images when there is an inflammation with necrosis, fibrosis or edema, due to the presence of accumulated contrast agent in the increased extracellular volume. On the other hand, the contrast on bSSFP images depends on the T2/T1 ratio where presence of edema in the myocardial tissue will result in a higher signal, due to the prolonged transverse relaxation (T2) time in the edematous tissue [16]. Presence of scars will result in a lower signal, due to a prolonged longitudinal relaxation (T1) time. Thus, active inflammation, in which edema is an important hallmark, will appear bright on bSSFP images. However, the signal will decrease when the inflammatory response leads to progressive fibrosis. Therefore, this imaging technique may in the future be a useful tool to determine if LGE on delayed images is indicating an active inflammation and/or progressive fibrosis. Future studies are needed to substantiate this hypothesis.

In order to demonstrate the potential of TA for the diagnosis of myocarditis, the study-design was set up to ensure successful separation in features between patients with detectable and non-detectable pathology. The features, which we expected to be important, included two first-order histogram features, *Variance* and *Skewness*, one first-order gradient-based feature, *Gradient Mean*, and one second-order co-occurrence-based feature, *Sum Average*. That is, these important features were expected to differentiate patients (group 1) from controls (group 3), as they reflect measures that are characteristic for visible pathology. With this study design, we have extracted features that have potential to be used in clinical practice for automated diagnosis of myocarditis, with the potential to present continuous quantitative information for longitudinal follow-up and possibly even for myocarditis phenotyping.

4.1 Study limitations

Our study population was relatively small with variations in demographic characteristics between the groups. However, we considered the sample size sufficient for a proof-of-concept study. Future studies should be performed using a larger sample size to further investigate the true potential of texture features, alone and combined, in order to detect and differentiate between different stages of myocarditis.

Compared to the previous study [8], our study design had different inclusion criteria of the control group due to the retrospective nature of the study design, making the comparison of the results difficult. In particular, the mean age was higher in the control group and this must be taken into consideration as this may have limited the possibility to separate the groups. Regardless, TA managed to differentiate between groups showing the potential of the method.

5. Conclusions

In conclusion, our study indicates that TA is feasible based on conventional bSSFP, LGE and T2-weighted CMRI, enabling automated detection of myocarditis in patients with initial clinical suspicion. The results showed statistical significance for *Variance*, *Skewness*, *Gradient Mean* and *Sum Average* based on LGE imaging between patients with and without proven myocarditis based on myocardial biomarkers and CMRI according to LLC. Except for *Skewness*, bSSFP imaging could also significantly differentiate between the presence and absence of myocarditis, emphasizing the potential of this non-contrast technique and its currently underappreciated value for tissue characterization. With T2-weighted imaging, only *Sum Average* and *Skewness* could significantly separate the two groups, explained by the lower contrast between normal and injured myocardium.

6. Acknowledgements

I would like to express my deepest gratitude to my supervisor Kerstin Lagerstrand, for inspiring me and giving me great support and encouragement throughout this project.

I would also like to thank Christian Polte for his help and feedback on this report.

Finally, many thanks to Dennis Lipničević for letting me ask countless questions.

Reference list

1. Cooper, L. T. Jr. Clinical manifestations and diagnosis of myocarditis in adults. UpToDate. 2018. Available at: https://www.uptodate.com/contents/clinical-manifestations-and-diagnosis-of-myocarditis-in-adults (Assessed 2018-09-10).
2. Sagar, S., Liu, P. P. & Cooper L. T. Jr. Myocarditis. Lancet. 2012; 379(9817): 738-47.
3. Friedrich, M. G. *et al.* International consensus group on cardiovascular magnetic resonance in myocarditis. J Am Coll Cardiol. 2009; 53(17): 1475-87.
4. Franco, A., Javidi, S. & Ruehm, S. G. Delayed myocardial enhancement in cardiac magnetic resonance imaging. J Radiol Case Rep. 2015; 9(6): 6-18.
5. McRobbie, D. W., Moore, E. A., Graves, M. J. & Prince, M. R. MRI from picture to proton. Cambridge University Press, Cambridge, United Kingdom. Third Edition. 2017; 269-287.
6. Castellano, G., Bonilha, L., Li, L. M. & Cendes, F. Texture analysis of medical images. Clin Radiol. 2004; 59(12): 1061-9.
7. Baeßler, B., Mannil, M., Maintz, D., Alkadhi, H. & Manka, R. Texture analysis and machine learning of non-contrast T1-weighted MR images in patients with hypertrophic cardiomyopathy—Preliminary results. Eur J Radiol. 2018; 102: 61-67.
8. Baeßler, B. *et al.* Cardiac MRI texture analysis of T1 and T2 maps in patients with infarctlike acute myocarditis. Radiology. 2018; 289(2): 357-365.
9. Szczypinski, P., Strzelecki, M., Materka, A. & Klepaczko, A. MaZda-a software package for image texture analysis. Comput Methods Programs Biomed. 2009; 94(1): 66-76.
10. Szczypinski P., Strzelecki M., Materka A. MaZda - a software for texture analysis. Proc. of ISITC 2007. 2007; 245-249.
11. Strzelecki, M., Szczypinski, P., Materka, A. & Klepaczko, A. A software tool for automatic classification and segmentation of 2D/3D medical images. Nucl Instrum Methods Phys Res A. 2013; 702: 137-140.
12. MATLAB R2018b, The MathWorks, Inc., Natick, MA, U.S.A.
13. Cicchetti, D. V. Guidelines, criteria, and rules of thumb for evaluating normed and standardized assessment instruments in psychology. Psychol Assess. 1994; 6(4): 284-290.
14. Masson, S., Latini, R., Salio, M. & Fiordaliso, F. 2007. Cardiac fibrosis and aging. In: Mohammed, S., Razzaque, M. D., editors. Fibrogenesis: Cellular and molecular basis. Kluwer Academic/Plenum Publishers, New York, U.S.A. 2005; 97-103.
15. van Griethuysen, J. J. M., *et al*. Computational radiomics system to decode the radiographic phenotype. Cancer Res. 2017; 77(21): 104–107.
16. Montant, P., Sigovan, M., Revel, D. & Douek, P. MR imaging assessment of myocardial edema with T2 mapping. Diagn Interv Imaging. 2015; 96(9): 885-90.
17. Gillies, R. J., Kinahan, P. E. & Hricak, H. Radiomics: Images are more than pictures, they are data. Radiology. 2016; 278(2): 563-77.
18. Aerts, H. J. *et al.* Decoding tumour phenotype by noninvasive imaging using a quantitative radiomics approach. Nat Commun. 2014; 5: 4006.
19. Strzelecki, M. & Szczypinski, P. MaZda: User's Manual. Institute of Electronics, Technical University of Lodz, Lodz, Poland. Available at: http://www.eletel.p.lodz.pl/programy/mazda/download/mazda_manual.pdf (Assessed 2018-09-20).

Appendix A – Texture analysis

Radiomics is a relatively new field of medical studies that has shown promising results for improved accuracy in diagnosis, assessment of prognosis and prediction of treatment response [18]. It has originally emerged from oncology and can provide information of personalized medicine, where treatments are adapted to characteristics of the patient and tumor [17]. Moreover, research is also increasing in other applications, ranging from the detection of lesions and segmentation of anatomical structures, to differentiation between normal and pathological tissue in different organs such as the brain, lungs [6] and recently also the heart [7,8]. As a part of the process in radiomics, TA is used to detect tissue characteristics and describe the underlying texture [6]. This analysis is performed on extracted texture features that are computed with data-characterization algorithms, based on pixel interrelationships and grey-level patterns in an image.

In this study, the features were extracted with MaZda and derived from six main categories: histogram, absolute gradient, grey-level run-length matrix, grey-level co-occurrence matrix, auto-regressive model and wavelets. The texture categories with including texture features, computed by MaZda, are described below [6,15,18,19]. The mathematical definitions of these features can be found in the Mazda manual [19].

1. Histogram features
The histogram of an image will show the distribution of pixels with a given grey-level value. In a 12 bits image, the grey-level values range from 0 to 4095, with 0 representing black and 4095 white. The histogram contains first-order statistics of an image, without providing information about spatial relationships. Texture features computed by MaZda, derived from the histogram, are mean, variance, skewness, kurtosis and different percentiles.

2. Absolute gradient features
The gradient measures the spatial variation of the grey-level values in an image, where a big change between pixels gives a high gradient value and a small change gives a low gradient value. Computed parameters in Mazda, derived from the absolute gradient image, are mean, variance, skewness, kurtosis and the percentage of nonzero gradient pixels.

3. Run-length matrix features
The run-length matrix is searching across the image for runs of pixels with the same grey-level value. The length of the run is defined by the number of pixels within the run. The computed features by Mazda are run-length nonuniformity (RLNonUni), grey-level nonuniformity (GLevNonU), long-run emphasis (LngREmp), short-run emphasis (ShrtREmp) and fraction of image in runs. They are considered higher order parameters and the calculated direction of them are vertical, horizontal and diagonal in 45 degrees and 135 degrees.

4. Co-occurrence matrix features
The co-occurrence matrix contains information about the grey-level distribution of pairs of pixels and can be defined as the second-order histogram. With defined distances and directions, the co-occurrence matrix is calculated for each angle, where counts are made for the number of occurrences of given pixel grey-level values. With the mean of the calculated values on the matrix, for each angle, numeric features are then computed on the resultant matrix. Computed features by Mazda are angular second moment, contrast, correlation, sum of squares, inverse difference moment, sum average, sum variance, sum entropy, entropy, difference variance and difference entropy.

5. Auto-regressive model features
In the auto-regressive model, local interactions between pixels in an image are assumed. The grey-level values of the neighboring pixels around a pixel represents a weighted sum of the grey-level values in that pixel. Different relations between groups of neighboring pixels can be found and thus, shapes within the image can be described. The computed parameters are the set of weights and the standard deviation of the driving noise.

6. Wavelet-based features
Wavelets analyzes data of an image in different frequency components within different scales of the image. Computed wavelet parameters are energy of wavelet coefficients in low-frequency sub-bands, horizontal high-frequency sub-bands, vertical high-frequency sub-bands, and diagonal high-frequency sub-bands.

Appendix B – Supplementary results

Table 6. Estimated p-values for texture features between the different imaging techniques bSSFP, LGE and T2w.

Texture feature	Group 1		
	bSSFP – LGE	LGE – T2w	bSSFP – T2w
Gradient Mean	**0.002**	0.4	0.02
Sum Average	**0.002**	**0.003**	0.9
Skewness	**< 0.001**	**< 0.001**	0.9
Variance	**< 0.001**	0.09	**0.03**
GLevNonU (0°)	**0.03**	0.4	0.1
GLevNonU (45°)	**0.02**	0.5	0.1
GLevNonU (90°)	**0.03**	0.7	0.08
GLevNonU (135°)	**0.03**	0.5	0.1
RLNonUni (0°)	0.05	0.3	**0.006**
RLNonUni (45°)	**0.04**	0.1	**0.002**
RLNonUni (90°)	0.07	0.1	**0.002**
RLNonUni (135°)	0.06	0.2	**0.002**

bSSFP = balanced steady-state-free-precession, LGE = late gadolinium enhancement, T2w = T2-weighted imaging, GLevNonU = grey-level nonuniformity, RLNonUni = run-length nonuniformity. Statistically significant p-values are highlighted in **bold** (p < 0.05).

Table 7. For features extracted with bSSFP, LGE and T2-weighted imaging in the group with reanalyzed patients, the ICC-values were generally in the range 0.6 – 1.0, indicating good or excellent agreement in reproducibility.

Texture features	Group 1		
	bSSFP	LGE	T2w
Gradient Mean	0.98	0.98	0.99
Sum Average	0.48	0.87	0.90
Skewness	0.89	0.96	0.97
Variance	0.98	0.99	0.99
GLevNonU (0°)	0.91	0.87	0.90
GLevNonU (45°)	0.91	0.87	0.90
GLevNonU (90°)	0.91	0.86	0.90
GLevNonU (135°)	0.91	0.87	0.91
RLNonUni (0°)	0.66	0.81	0.86
RLNonUni (45°)	0.62	0.84	0.86
RLNonUni (90°)	0.62	0.85	0.87
RLNonUni (135°)	0.64	0.85	0.88

bSSFP = balanced steady-state-free-precession, LGE = late gadolinium enhancement, T2w = T2-weighted imaging, GLevNonU = grey-level nonuniformity, RLNonUni = run-length nonuniformity.